

# Measurement of the CKM angle $\alpha$ ( $\phi_2$ ) with $B \rightarrow \rho\rho$ decays at Belle and **BABAR**

A. Somov\*

University of Cincinnati, Cincinnati, Ohio, 45221, USA

We overview recent measurements in  $B \rightarrow \rho\rho$  decays which are based on data samples collected at the PEP-II and KEKB asymmetric-energy  $e^+e^-$  colliders with the **BABAR** and Belle detectors. Special emphasis is given to the determination of the  $CP$ -violating coefficients  $\mathcal{A}$  and  $\mathcal{S}$  from an analysis of  $B^0 \rightarrow \rho^+\rho^-$  decays. The values of  $\mathcal{A}$  and  $\mathcal{S}$ , branching fractions, and longitudinal polarization fractions of  $B \rightarrow \rho\rho$  decays are used to constrain the Cabibbo-Kobayashi-Maskawa phase  $\alpha(\phi_2)$  using an isospin analysis; the solution consistent with the standard model is  $71^\circ < \alpha(\phi_2) < 113^\circ$  at 68% C.L.

## I. INTRODUCTION

$CP$  violation in the Standard Model can be explained by the presence of an irreducible complex phase in the Cabibbo-Kobayashi-Maskawa [1] (CKM) quark-mixing matrix. The unitarity of the CKM matrix leads to six triangles in the complex plane. One such triangle is given by the following relation among the matrix elements:  $V_{ub}^*V_{ud} + V_{cb}^*V_{cd} + V_{tb}^*V_{td} = 0$ . The phase angle  $\phi_2^1$ , defined as  $\arg[-(V_{td}V_{tb}^*)/(V_{ud}V_{ub}^*)]$ , can be determined by measuring a time-dependent  $CP$  asymmetry in  $b \rightarrow u\bar{u}d$  decays such as  $B^0 \rightarrow \pi^+\pi^-$ ,  $\rho^\pm\pi^\mp$ , and  $\rho^+\rho^-$ . The time-dependent decay rate for  $B \rightarrow \rho^+\rho^-$  decays tagged with  $B^0$  ( $q = 1$ ) and  $\overline{B}^0$  ( $q = -1$ ) mesons is given by

$$\mathcal{P}_{\rho\rho}(\Delta t) = \frac{e^{-|\Delta t|/\tau_{B^0}}}{4\tau_{B^0}} \{1 + q[\mathcal{A}_{\rho\rho} \cos(\Delta m \Delta t) + \mathcal{S}_{\rho\rho} \sin(\Delta m \Delta t)]\}, \quad (1)$$

where  $\tau_{B^0}$  is the  $B^0$  lifetime,  $\Delta m$  is the mass difference between the two  $B^0$  mass eigenstates,  $\Delta t = t_{CP} - t_{tag}$ , and  $\mathcal{A}_{\rho\rho}$  (**BABAR**'s definition is  $\mathcal{C}_{\rho\rho} = -\mathcal{A}_{\rho\rho}$ ) and  $\mathcal{S}_{\rho\rho}$  are  $CP$  asymmetry coefficients to be obtained from a fit to the experimental data. If the decay amplitude is a pure  $CP$ -even state and is dominated by a tree diagram,  $\mathcal{S}_{\rho\rho} = \sin(2\phi_2)$  and  $\mathcal{A}_{\rho\rho} = 0$ . The presence of an amplitude with a different weak phase (such as from a "penguin" diagram) gives rise to direct  $CP$  violation and shifts  $\mathcal{S}_{\rho\rho}$  from  $\sin(2\phi_2)$ . However, the size of the loop amplitude is constrained by the branching fraction of  $B^0 \rightarrow \rho^0\rho^0$  [2], indicating that this effect is small.

The  $CP$ -violating parameters receive contributions from a longitudinally polarized state ( $CP$ -even) and two transversely polarized states (an admixture of  $CP$ -even and  $CP$ -odd states). Recent measurements of the polarization fraction by Belle and **BABAR** [3, 4] show that the longitudinal polarization fraction is approximately 100% ( $f_L = 0.968 \pm 0.023$  [5]).  $f_L$  can

be extracted from a fit to helicity-angle distribution. The angular decay rate  $d^2\Gamma/(\Gamma d\cos\theta_+ d\cos\theta_-)$  is given by  $\frac{9}{4} \{f_L \cos^2\theta_+ \cos^2\theta_- + \frac{1}{4}(1-f_L) \sin^2\theta_+ \sin^2\theta_-\}$ , where,  $\theta_\pm$  is the angle between the direction of the  $\pi^0$  from the  $\rho^\pm$  and the negative of the  $B^0$  momentum in the  $\rho^\pm$  rest frame.

## II. MEASUREMENTS

The common features of  $B \rightarrow \rho\rho$  analyses are: (1) relatively small signal yields; the branching fractions of  $B \rightarrow \rho\rho$  decays are in the order of  $10^{-6} - 10^{-5}$ , (2) large width of  $\rho$  mesons results in the large background; the fraction of signal events in most analysis is less than 1%, (3) there are several background sources:  $e^+e^- \rightarrow q\bar{q}$  ( $q = u, d, s, c$ ) continuum,  $b \rightarrow c$ , and  $b \rightarrow u$  backgrounds, (4) significant amount of events with multiple reconstructed  $B$  candidates, (5) various variables are used in the likelihood functions to distinguish among signal and backgrounds.

Both Belle and **BABAR** analyses identify  $B \rightarrow \rho\rho$  decays using the beam-energy constrained mass  $M_{bc} \equiv \sqrt{E_{beam}^2 - p_B^2}$  (called as beam-energy-substituted mass,  $m_{ES}$ , in **BABAR**) and energy difference  $\Delta E \equiv E_B - E_{beam}$ , where  $E_{beam}$  is the beam energy, and  $E_B$  and  $p_B^2$  are the energy and momentum of the reconstructed  $B$  candidate, all evaluated in the center-of-mass (CM) frame.

The dominant background originates from  $e^+e^- \rightarrow q\bar{q}$  ( $q = u, d, s, c$ ) continuum events. To separate  $q\bar{q}$  jet-like events from spherical-like  $B\bar{B}$  events, Belle uses event-shape variables, specifically, modified Fox-Wolfram moments combined into a Fisher discriminant [6], and  $\theta_B$ , the polar angle in the CM frame between the  $B$  direction and the beam axis. The Fisher discriminant and  $\theta_B$  are used to form a ratio of signal and background likelihoods  $\mathcal{R}$ . In the  $B^\pm \rightarrow \rho^\pm\rho^0$  analysis Belle also requires  $|\cos\theta_T| < 0.8$ , where  $\theta_T$  is the angle between the thrust axis of the candidate tracks and that of the remaining tracks in the event. In the **BABAR** analyses  $q\bar{q}$  background is suppressed by requiring  $|\cos\theta_T| < 0.8$  and making use of a neural network discriminant  $\mathcal{N}$  which is based on several event-shape variables. Below we describe  $B \rightarrow \rho\rho$  measurements in detail.

\*Electronic address: somov@physics.uc.edu

<sup>1</sup> The naming convention: angles  $\alpha$ ,  $\beta$ , and  $\gamma$  used in **BABAR** are referred to as  $\phi_2$ ,  $\phi_1$ , and  $\phi_3$  in Belle.

TABLE I: Reconstruction requirements used in  $B^0 \rightarrow \rho^+ \rho^-$  analysis. The barrel and (endcap) regions in the electromagnetic calorimeter at Belle are defined as  $32^\circ < \theta < 129^\circ$  and  $(17^\circ < \theta < 32^\circ$  and  $129^\circ < \theta < 150^\circ$ ), where  $\theta$  denotes the polar angle with respect to the beam axis.

Cut	BABAR	Belle
$E_\gamma$ (MeV)	50	50 (barrel) 90 (endcap)
$M_{\gamma\gamma}$ (MeV/c <sup>2</sup> )	100. - 160.	117.8 - 150.2
$M_{\pi^\pm \pi^0}$ (GeV/c <sup>2</sup> )	0.5 - 1.0	0.62 - 0.92
$\cos \theta_\pm$	-0.9 - 0.98	-0.8 - 0.98
$M_{bc}$ (GeV/c <sup>2</sup> )	5.25 - 5.29	5.23 - 5.29
$\Delta E$ (GeV)	-0.12 - 0.15	-0.2 - 0.3
		-0.12 - 0.08 ( <i>CP</i> fit)

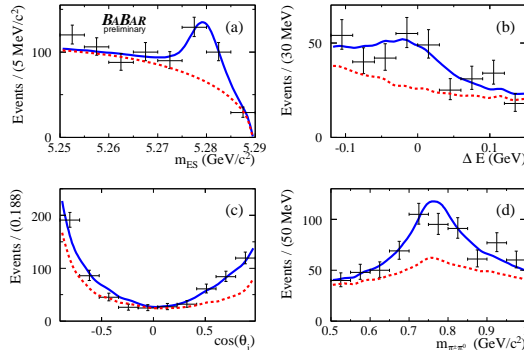


FIG. 1: *BABAR* (a)  $m_{ES}$ , (b)  $\Delta E$ , (c)  $\cos \theta$ , and (d)  $m_{\pi^\pm \pi^0}$  for the highest purity tagged events. The curves show fit projections: the dashed line is background and the solid line is the total.

### A. $B^0 \rightarrow \rho^+ \rho^-$

$B^0 \rightarrow \rho^+ \rho^-$  decays are reconstructed by combining two oppositely charged pion tracks with two neutral pions. The  $\rho^\pm$  mesons are selected combining  $\pi^\pm$  with  $\pi^0$  candidates. The  $\pi^0$  candidates are reconstructed from  $\gamma\gamma$  pairs. Main event reconstruction requirements are listed in Table I. A flavor of the  $B$  meson accompanying the  $B^0 \rightarrow \rho^+ \rho^-$  candidate is identified via its decay products. Tagging algorithms yield the flavor of the tagged meson and a flavor-tagging quality. In events with multiple reconstructed  $B$  candidates the best candidate is selected based on the  $\pi^0$  masses, i.e. minimizing  $\sum_{\pi_{1,2}^0} (m_{\gamma\gamma} - m_{\pi^0})^2$ . The fraction of signal decays which have at least one  $\pi^\pm$  track incorrectly identified but pass all selection criteria is 13.8% and 6.5% for *BABAR* and *Belle*, respectively. These are referred to as “self-cross-feed” (SCF) events. The following components are distinguished in the analyses: signal and  $\rho\pi\pi$  non-resonant decays, SCF events, continuum background ( $q\bar{q}$ ), charm  $B$  background ( $b \rightarrow c$ ), and charmless ( $b \rightarrow u$ ) background. The  $b \rightarrow u$  background is dominated by  $B \rightarrow (\rho\pi, a_1\pi, a_1\rho, \rho^\pm\rho^0)$  decays.

*BABAR* obtains the signal yield,  $f_L$ , and *CP*-violating

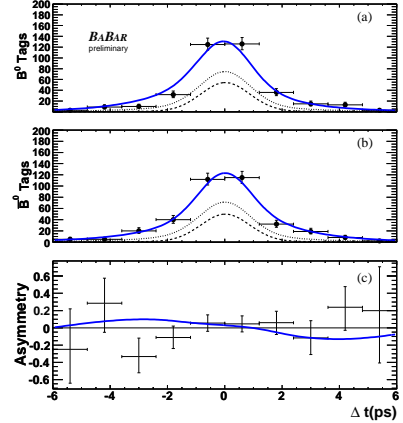


FIG. 2: *BABAR* the  $\Delta t$  distributions of a signal-enriched sample for (a)  $B^0$  and (b)  $\bar{B}^0$  tagged events. (c) shows raw asymmetry. The dashed lines denote  $q\bar{q}$  background, the dotted lines are the sum of background, and the solid lines are the total.

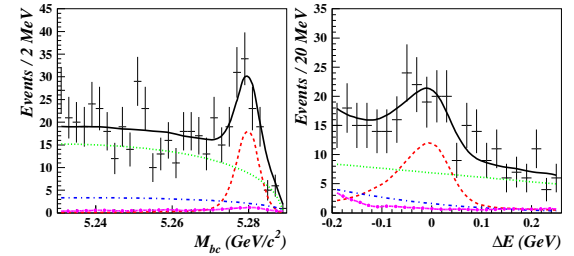


FIG. 3: *Belle*: projections in  $M_{bc}$  (left) and  $\Delta E$  (right) for the high-purity tagged events of a sample enriched in signal. The curves show fit projections: dashed is  $\rho^+ \rho^- + \rho\pi\pi$ , dotted is  $q\bar{q}$ , dot-dashed is  $b \rightarrow c$ , long-dashed is  $b \rightarrow u$ , and solid is the total.

parameters  $\mathcal{A}_{\rho^+ \rho^-}$  and  $\mathcal{S}_{\rho^+ \rho^-}$  from an unbinned extended maximum-likelihood (ML) fit to  $m_{ES}$ ,  $\Delta E$ ,  $\Delta t$ ,  $m_{\pi^\pm \pi^0}$ ,  $\cos \theta_\pm$ , and  $\mathcal{N}$  distribution of 33902 events [7].

The *Belle* analysis is organized in two main steps: (a) we first determine the yields of signal and background components from an unbinned extended ML fit to the three-dimensional  $M_{bc}$  -  $\Delta E$  -  $\mathcal{R}$  distribution. (b) we perform a fit to the  $\Delta t$  distribution of 18004 events to determine the *CP* parameters  $\mathcal{A}_{\rho^+ \rho^-}$  and  $\mathcal{S}_{\rho^+ \rho^-}$ . The fit results are presented in Figures 1, 2, 3, and 4 and are listed in Table III. The fraction of longitudinal polarization and fraction of non-resonant events ( $6.3 \pm 6.7\%$ ) were measured in our previous analysis [3]. The branching fraction,  $f_L$ , and *CP* asymmetries measured by *Belle* are similar to those obtained by *BABAR*. The values  $\mathcal{A}_{\rho^+ \rho^-}$  and  $\mathcal{S}_{\rho^+ \rho^-}$  are also consistent with no *CP* violation ( $\mathcal{A} = \mathcal{S} = 0$ ).

### B. $B^\pm \rightarrow \rho^\pm \rho^0$

The main reconstruction features of the analysis are the same as those for the  $B^0 \rightarrow \rho^+ \rho^-$ . Event selection requirements are listed in Table II.

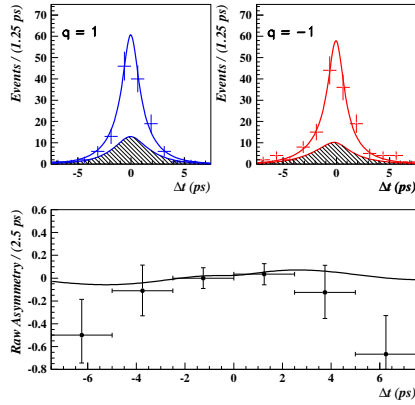


FIG. 4: Belle: the  $\Delta t$  distribution and projections of the fit for high-purity tagged events: (a)  $B^0$  tags, (b)  $\bar{B}^0$  tags. The raw  $CP$  asymmetry is shown in (c). The hatched region shows signal events.

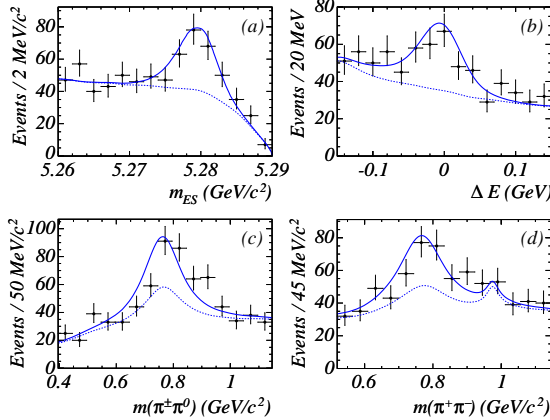


FIG. 5: BABAR (a)  $m_{ES}$ , (b)  $\Delta E$ , (c)  $\cos \theta$ , and (d)  $m_{\pi^\pm \pi^0}$  distributions for a signal-enriched samples along with fit projections: the dashed lines show  $q\bar{q}$  and  $B\bar{B}$  backgrounds, the solid line is the total.

BABAR obtained the yields of  $B^\pm \rightarrow \rho^\pm \rho^0$  and  $B^\pm \rightarrow \rho^\pm f_0$  decays, polarization, and charge asymmetry  $\mathcal{A}_{\rho^\pm \rho^0} = (N_{B^-} - N_{B^+})/(N_{B^-} + N_{B^+})$  using an unbinned extended ML fit to  $m_{ES}$ ,  $\Delta E$ ,  $\Delta t$ ,  $m_{\pi^\pm \pi^0}$ ,  $m_{\pi^+ \pi^-}$ ,  $\cos \theta_\pm$ ,  $\cos \theta_0$ , and  $\mathcal{N}$  distribution of 74293 events [8]. The charmless  $b \rightarrow u$  background is dominated by  $\eta' \rho^\pm$ ,  $K^{*0} \rho^\pm$ ,  $a_1^\pm \pi^\pm$ ,  $a_1^\pm \pi^0$ ,  $a_1^\pm \rho^0$ , and  $a_1^\pm \rho^\pm$  decays.

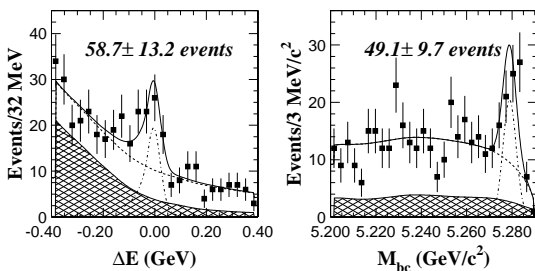


FIG. 6: Belle:  $\Delta E$  (left) and  $M_{bc}$  (right) distributions. The dashed curve is the sum of  $B\bar{B}$  and continuum backgrounds, the dot-dashed curve is the signal, the hatched region shows  $B\bar{B}$ , and the solid curve is the total.

TABLE II: Reconstruction requirements used in  $B^\pm \rightarrow \rho^\pm \rho^0$  analysis.

Cut	BABAR	Belle
$E_\gamma$ (MeV)	50	50 (barrel); 100 (endcap)
$M_{\gamma\gamma}$ (MeV/c <sup>2</sup> )	100. - 160.	118. - 150.
$M_{\pi^\pm \pi^0}$ (GeV/c <sup>2</sup> )	0.396 - 1.146	0.65 - 0.89
$M_{\pi^+ \pi^-}$ (GeV/c <sup>2</sup> )	0.520 - 1.146	0.65 - 0.89
$\cos \theta_\pm$	-0.9 - 0.95	-
$\cos \theta_0$	-0.95 - 0.95	-
$p_{\pi^0}^{CM}$ (GeV/c)		> 0.5
$M_{bc}$ (GeV/c <sup>2</sup> )	5.26 <	5.272 <
$\Delta E$ (GeV)	-0.15 - 0.15	-0.4 - 0.4

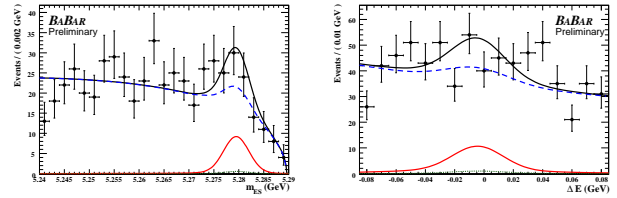


FIG. 7: BABAR  $m_{ES}$  and  $\Delta E$  distributions and projections of the fit for a signal-enriched sample. The dashed curve is full background, the small solid curve is signal, the dotted curve is  $B \rightarrow \rho^0 f_0$ , and the large solid is the total.

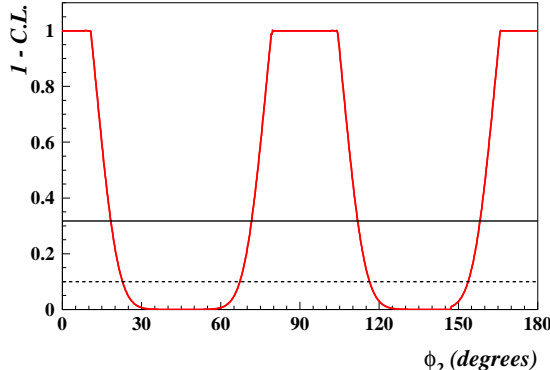
The signal yield in Belle analysis [9] is obtained from a fit to  $\Delta E$  distribution. To measure the polarization, Belle bins in  $\cos \theta_\pm$  and  $\cos \theta_0$  and determine the signal yield for each bin from the fit to  $\Delta E$  distribution. The polarization is obtained from a simultaneous fit to two background-subtracted helicity-angle distributions. The results of the fits are shown in Figures 5 and 6 and listed in Table III.

### III. $B^0 \rightarrow \rho^0 \rho^0$

BABAR finds evidence for  $B^0 \rightarrow \rho^0 \rho^0$  decays and measures its branching fraction and polarization using a sample of about 348 million  $B\bar{B}$  pairs [2]. Events are selected from the region  $5.24 \text{ GeV}/c^2 < M_{bc} < 5.29 \text{ GeV}/c^2$ ,  $|\Delta E| < 85 \text{ MeV}$ , and are required to satisfy  $0.55 < M_{\pi^+ \pi^-} < 1.05 \text{ GeV}/c^2$ , and  $|\cos \theta_0| < 0.98$ . In events with multiple  $B$  candidates one is selected based on the best  $\chi^2$  of a four-pion vertex fit. Additional suppression of the dominant continuum background is achieved using the flavor tagging information. The data sample is divided into seven tag-quality intervals,  $c_{tag}$ . The  $B^0 \rightarrow \rho^0 \rho^0$  event yield and polarization  $f_L$  are obtained from an unbinned extended ML fit to  $m_{ES}$ ,  $\Delta E$ ,  $m_{\pi^+ \pi^- 1,2}$ ,  $\cos \theta_{1,2}$ ,  $\mathcal{N}$ , and  $c_{tag}$  distribution of 65180 events. The fit also allows to obtain the yields for  $B^0 \rightarrow \rho^0 f_0(990)$  and  $B^0 \rightarrow f_0(980) f_0(980)$  decays. The charmless background is dominated by  $B^0 \rightarrow a_1^\pm \pi^\mp$  events which number is a free parameter in the fit. Other  $b \rightarrow u$  background modes include:  $B \rightarrow (\rho^0 K^{*0}, \rho^+ \rho^0, \rho \pi)$ , and  $B^0 \rightarrow \rho^+ \rho^-$ . The fit results are shown in Fig. 7 and listed in Table III.

TABLE III: Summary of  $B \rightarrow \rho\rho$  measurements.

Decay	Quantity	BABAR				Belle			HFAG
		Value	$N_{sig}$	$\mathcal{L}(\text{fb}^{-1})$	Value	$N_{sig}$	$\mathcal{L}(\text{fb}^{-1})$		
$B \rightarrow \rho^\pm \rho^\mp$	$\text{Br} (10^{-6})$	$23.5 \pm 2.2 \pm 4.1$	$615 \pm 57$	316	$22.8 \pm 3.8^{+2.3}_{-2.6}$	$194 \pm 32$	253	$23.1^{+3.2}_{-3.3}$	
	$f_L$	$0.977 \pm 0.024^{+0.015}_{-0.013}$	$615 \pm 57$	316	$0.941^{+0.034}_{-0.040} \pm 0.030$	$194 \pm 32$	253	$0.968 \pm 0.23$	
	$\mathcal{A}_{\rho^+\rho^-}$	$0.07 \pm 0.15 \pm 0.06$	$615 \pm 57$	316	$0.16 \pm 0.21 \pm 0.07$	$372 \pm 43$	492	$0.11 \pm 0.13$	
	$\mathcal{S}_{\rho^+\rho^-}$	$-0.19 \pm 0.21^{+0.05}_{-0.07}$	$615 \pm 57$	316	$0.19 \pm 0.30 \pm 0.07$	$372 \pm 43$	492	$-0.06 \pm 0.18$	
$B \rightarrow \rho^\pm \rho^0$	$\text{Br} (10^{-6})$	$16.8 \pm 2.2 \pm 2.3$	$390 \pm 49$	210.5	$31.7 \pm 7.1^{+3.8}_{-6.7}$	$58.7 \pm 13.2$	78	$18.2 \pm 3.0$	
	$f_L$	$0.905 \pm 0.042^{+0.023}_{-0.027}$	$390 \pm 49$	210.5	$0.948 \pm 0.106 \pm 0.021$	$58.7 \pm 13.2$	78	$0.912^{+0.044}_{-0.045}$	
	$\mathcal{A}_{\rho^\pm \rho^0}$	$-0.12 \pm 0.13 \pm 0.10$	$390 \pm 49$	210.5	$0.00 \pm 0.22 \pm 0.03$	$58.7 \pm 13.2$	78	$-0.08 \pm 0.13$	
$B \rightarrow \rho^0 \rho^0$	$\text{Br} (10^{-6})$	$1.16^{+0.37}_{-0.36} \pm 0.27$	$98^{+32}_{-31}$	316				$1.16 \pm 0.46$	
	$f_L$	$0.86^{+0.11}_{-0.13} \pm 0.05$	$98^{+32}_{-31}$	316				$0.86^{+0.12}_{-0.14}$	

FIG. 8: 1 - C.L. vs.  $\phi_2$ . The horizontal lines denote C.L. = 68.3% (solid) and C.L. = 90% (dashed)

#### IV. CONSTRAINT ON $\alpha(\phi_2)$

We constrain  $\phi_2$  using an isospin analysis [10], which allows one to relate six observables to six underlying parameters: five decay amplitudes for  $B \rightarrow \rho\rho$  and the angle  $\phi_2$ . The observables are the branching fractions for  $B \rightarrow \rho^+ \rho^-$ ,  $\rho^+ \rho^0$ , and  $\rho^0 \rho^0$  (listed in Table III) [5]; the  $CP$  parameters  $\mathcal{A}_{\rho^+ \rho^-}$  and  $\mathcal{S}_{\rho^+ \rho^-}$ ; and the parameter

$\mathcal{A}_{\rho^0 \rho^0}$  for  $B \rightarrow \rho^0 \rho^0$  decays. The branching fractions must be multiplied by the corresponding longitudinal polarization fractions (taken from Table III) [5]. We neglect possible contributions from electroweak penguins and  $I=1$  amplitudes [11] to  $B^0 \rightarrow \rho^+ \rho^-$ . We follow the statistical method of Ref. [12] and construct a  $\chi^2(\phi_2)$  using the measured values and obtain a minimum  $\chi^2$  (denoted  $\chi^2_{\min}$ ); we then scan  $\phi_2$  from  $0^\circ$  to  $180^\circ$ , calculating the difference  $\Delta\chi^2 \equiv \chi^2(\phi_2) - \chi^2_{\min}$ . We insert  $\Delta\chi^2$  into the cumulative distribution function for the  $\chi^2$  distribution for one degree of freedom to obtain a confidence level (C.L.) for each  $\phi_2$  value. The resulting function  $1 - \text{C.L.}$  (Fig. 8) has more than one peak due to ambiguities that arise when solving for  $\phi_2$ . Because  $\mathcal{A}_{\rho^0 \rho^0}$  is not yet measured, we allow this observable to float; this produces the “flat-top” regions in Fig. 8. The solution consistent with the Standard Model is  $71^\circ < \phi_2 < 113^\circ$  at 68% C.L. or  $67^\circ < \phi_2 < 116^\circ$  at 90% C.L. Recently, a different model-dependent approach to extract  $\phi_2$  using flavor  $SU(3)$  symmetry has been proposed [13]. This method would give more stringent constraints on  $\phi_2$ .

In summary, we present recent measurements in  $B \rightarrow \rho\rho$  decays. These measurements are used to constrain the angle  $\phi_2$  using an isospin analysis.

---

[1] M. Kobayashi and T. Maskawa, Prog. Theor. Phys. **49**, 652 (1973); N. Cabibbo, Phys. Rev. Lett. **10**, 531 (1963).  
[2] B. Aubert *et al.*, Phys. Rev. Lett. **94**, 131801 (2005); hep-ex/0612021 (2006), submitted to Phys. Rev. Lett.  
[3] A. Somov *et al.*, Phys. Rev. Lett. **96**, 171801 (2006).  
[4] B. Aubert *et al.*, Phys. Rev. Lett. **95**, 041805 (2005); Phys. Rev. Lett. **93**, 231801 (2004).  
[5] Heavy Flavor Averaging Group, August 2006, <http://www.slac.stanford.edu/xorg/hfag/>.  
[6] S. H. Lee *et al.*, Phys. Rev. Lett. **91**, 261801 (2003).  
[7] B. Aubert *et al.*, hep-ex/0607098.  
[8] B. Aubert *et al.*, Phys. Rev. Lett. **97**, 261801 (2006).  
[9] J. Zhang *et al.*, Phys. Rev. Lett. **91**, 221801 (2003).  
[10] M. Gronau, D. London, Phys. Rev. Lett. **65**, 3381 (1990).  
[11] A. Falk *et al.*, Phys. Rev. D **69**, 011502(R) (2004).  
[12] J. Charles *et al.*, Eur. Phys. J. C41, 1 (2005).  
[13] M. Beneke, M. Gronau, J. Rohrer and M. Spranger, Phys. Lett. B **638**, 68 (2006).